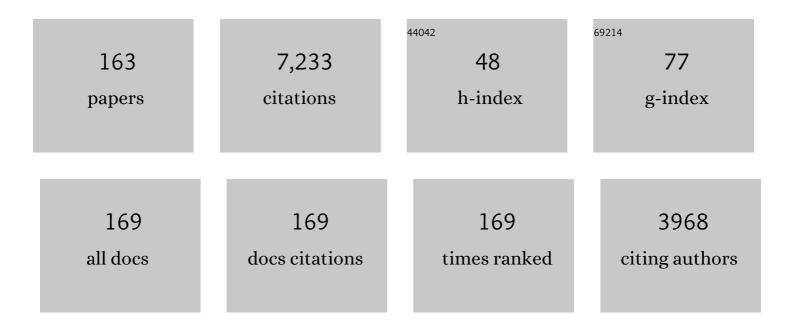
List of Publications by Year in descending order

Source: https://exaly.com/author-pdf/8735251/publications.pdf Version: 2024-02-01



YUNZHI MANC

#	Article	IF	CITATIONS
1	Phase field modeling of defects and deformation. Acta Materialia, 2010, 58, 1212-1235.	3.8	365
2	Development of low-alloyed and rare-earth-free magnesium alloys having ultra-high strength. Acta Materialia, 2018, 149, 350-363.	3.8	287
3	Giant strain with low hysteresis in A-site-deficient (Bi0.5Na0.5)TiO3-based lead-free piezoceramics. Acta Materialia, 2017, 128, 337-344.	3.8	222
4	Role of ω phase in the formation of extremely refined intragranular α precipitates in metastable β-titanium alloys. Acta Materialia, 2016, 103, 850-858.	3.8	201
5	In situ design of advanced titanium alloy with concentration modulations by additive manufacturing. Science, 2021, 374, 478-482.	6.0	168
6	Grain growth in anisotropic systems: comparison of effects of energy and mobility. Acta Materialia, 2002, 50, 2491-2502.	3.8	161
7	Quantitative phase field modeling of diffusion-controlled precipitate growth and dissolution in Ti–Al–V. Scripta Materialia, 2004, 50, 471-476.	2.6	153
8	Strain glass in Fe-doped Ti–Ni. Acta Materialia, 2010, 58, 6206-6215.	3.8	152
9	Incorporation of γ-surface to phase field model of dislocations: simulating dislocation dissociation in fcc crystals. Acta Materialia, 2004, 52, 683-691.	3.8	142
10	Variant selection of grain boundary α by special prior β grain boundaries in titanium alloys. Acta Materialia, 2014, 75, 156-166.	3.8	142
11	Effect of Ni4Ti3 precipitation on martensitic transformation in Ti–Ni. Acta Materialia, 2010, 58, 6685-6694.	3.8	140
12	Variant selection during α precipitation in Ti–6Al–4V under the influence of local stress – A simulation study. Acta Materialia, 2013, 61, 6006-6024.	3.8	129
13	Modeling Abnormal Strain States in Ferroelastic Systems: The Role of Point Defects. Physical Review Letters, 2010, 105, 205702.	2.9	128
14	Phase field model of dislocation networks. Acta Materialia, 2003, 51, 2595-2610.	3.8	127
15	Formation mechanisms of self-organized core/shell and core/shell/corona microstructures in liquid droplets of immiscible alloys. Acta Materialia, 2013, 61, 1229-1243.	3.8	122
16	The indirect influence of the ω phase on the degree of refinement of distributions of the α phase in metastable β-Titanium alloys. Acta Materialia, 2016, 103, 165-173.	3.8	111
17	Large-scale three-dimensional phase field simulation of γ ′-rafting and creep deformation. Philosophical Magazine, 2010, 90, 405-436.	0.7	98
18	On variant distribution and coarsening behavior of the α phase in a metastable β titanium alloy. Acta Materialia, 2016, 106, 374-387.	3.8	98

#	Article	IF	CITATIONS
19	Kinetics of tweed and twin formation during an ordering transition in a substitutional solid solution. Philosophical Magazine Letters, 1992, 65, 15-23.	0.5	93
20	The role of the ω phase on the non-classical precipitation of the α phase in metastable β-titanium alloys. Scripta Materialia, 2016, 111, 81-84.	2.6	93
21	Effect of elastic interaction on nucleation: II. Implementation of strain energy of nucleus formation in the phase field method. Acta Materialia, 2007, 55, 1457-1466.	3.8	89
22	An integrated full-field model of concurrent plastic deformation and microstructure evolution: Application to 3D simulation of dynamic recrystallization in polycrystalline copper. International Journal of Plasticity, 2016, 80, 38-55.	4.1	89
23	Phase field modeling of channel dislocation activity and γ′ rafting in single crystal Ni–Al. Acta Materialia, 2007, 55, 5369-5381.	3.8	88
24	Microstructural Development of Coherent Tetragonal Precipitates in Magnesium-Partially-Stabilized Zirconia: A Computer Simulation. Journal of the American Ceramic Society, 1995, 78, 657-661.	1.9	86
25	Simulation study of precipitation in an Mg–Y–Nd alloy. Acta Materialia, 2012, 60, 4819-4832.	3.8	84
26	Superelasticity of slim hysteresis over a wide temperature range by nanodomains of martensite. Acta Materialia, 2014, 66, 349-359.	3.8	81
27	Heterogeneously randomized STZ model of metallic glasses: Softening and extreme value statistics during deformation. International Journal of Plasticity, 2013, 40, 1-22.	4.1	78
28	Strain glass transition in a multifunctional Î ² -type Ti alloy. Scientific Reports, 2014, 4, 3995.	1.6	76
29	Shape evolution of a precipitate during strain-induced coarsening. Scripta Metallurgica Et Materialia, 1991, 25, 1387-1392.	1.0	74
30	Multi-scale phase field approach to martensitic transformations. Materials Science & Engineering A: Structural Materials: Properties, Microstructure and Processing, 2006, 438-440, 55-63.	2.6	69
31	Effect of elastic interaction on nucleation: I. Calculation of the strain energy of nucleus formation in an elastically anisotropic crystal of arbitrary microstructure. Acta Materialia, 2006, 54, 5617-5630.	3.8	67
32	Diffusive molecular dynamics and its application to nanoindentation and sintering. Physical Review B, 2011, 84, .	1.1	67
33	Microstructural and micromechanical evolution during dynamic recrystallization. International Journal of Plasticity, 2018, 100, 52-68.	4.1	66
34	Interaction of Trace Rareâ€Earth Dopants and Nanoheterogeneities Induces Giant Magnetostriction in Feâ€Ga Alloys. Advanced Functional Materials, 2018, 28, 1800858.	7.8	64
35	A phase field study of microstructural changes due to the Kirkendall effect in two-phase diffusion couples. Acta Materialia, 2001, 49, 3401-3408.	3.8	63
36	Transformation-induced elastic strain effect on the precipitation kinetics of ordered intermetallics. Philosophical Magazine Letters, 1991, 64, 241-251.	0.5	62

#	Article	IF	CITATIONS
37	A simulation study of β 1 precipitation on dislocations in an Mg–rare earth alloy. Acta Materialia, 2014, 77, 133-150.	3.8	60
38	Shape Evolution of a Coherent Tetragonal Precipitate in Partially Stabilized Cubic ZrO2: A Computer Simulation. Journal of the American Ceramic Society, 1993, 76, 3029-3033.	1.9	57
39	Solute segregation transition and drag force on grain boundaries. Acta Materialia, 2003, 51, 3687-3700.	3.8	57
40	Modeling displacive–diffusional coupled dislocation shearing of γ′ precipitates in Ni-base superalloys. Acta Materialia, 2011, 59, 3484-3497.	3.8	57
41	New intrinsic mechanism on gum-like superelasticity of multifunctional alloys. Scientific Reports, 2013, 3, 2156.	1.6	57
42	Predicting structure and energy of dislocations and grain boundaries. Acta Materialia, 2014, 74, 125-131.	3.8	54
43	Growth behavior of <mml:math <br="" altimg="si1.gif" xmlns:mml="http://www.w3.org/1998/Math/MathML">overflow="scroll"><mml:mrow><mml:mi>l³</mml:mi><mml:mo>'</mml:mo><mml:mo>/</mml:mo>/<ml:mi>l³ coprecipitates in Ni-Base superalloys. Acta Materialia, 2019, 164, 220-236.</ml:mi></mml:mrow></mml:math>	<td>i>≺rā≄nl:mo></td>	i>≺r ā≄nl: mo>
44	Enabling Large Superalloy Parts Using Compact Coprecipitation of γ′ and γ′′. Metallurgical and Materia Transactions A: Physical Metallurgy and Materials Science, 2018, 49, 708-717.	als 1.1	53
45	Phase diagram of polar states in doped ferroelectric systems. Physical Review B, 2012, 86, .	1.1	52
46	Taming martensitic transformation via concentration modulation at nanoscale. Acta Materialia, 2017, 130, 196-207.	3.8	52
47	Shuffle-nanodomain regulated strain glass transition in Ti-24Nb-4Zr-8Sn alloy. Acta Materialia, 2020, 186, 415-424.	3.8	52
48	P-phase precipitation and its effect on martensitic transformation in (Ni,Pt)Ti shape memory alloys. Acta Materialia, 2012, 60, 1514-1527.	3.8	50
49	Microstructure Map for Self-Organized Phase Separation during Film Deposition. Physical Review Letters, 2012, 109, 086101.	2.9	49
50	Group theory description of transformation pathway degeneracy in structural phase transformations. Acta Materialia, 2016, 109, 353-363.	3.8	49
51	Effect of low-angle grain boundaries on morphology and variant selection of grain boundary allotriomorphs and WidmanstAtten side-plates. Acta Materialia, 2016, 112, 347-360.	3.8	47
52	Finding Critical Nucleus in Solid-State Transformations. Metallurgical and Materials Transactions A: Physical Metallurgy and Materials Science, 2008, 39, 976-983.	1.1	46
53	Quantification of rafting of γ′ precipitates in Ni-based superalloys. Acta Materialia, 2016, 103, 322-333.	3.8	46
54	Shearing of γ' particles in Co-base and Co-Ni-base superalloys. Acta Materialia, 2018, 161, 99-109.	3.8	45

#	Article	IF	CITATIONS
55	Nano-scale structural non-uniformities in gum like Ti-24Nb-4Zr-8Sn metastable β-Ti alloy. Scripta Materialia, 2019, 158, 95-99.	2.6	45
56	The role of nano-scaled structural non-uniformities on deformation twinning and stress-induced transformation in a cold rolled multifunctional β-titanium alloy. Scripta Materialia, 2020, 177, 181-185.	2.6	45
57	Direct determination of structural heterogeneity in metallic glasses using four-dimensional scanning transmission electron microscopy. Ultramicroscopy, 2018, 195, 189-193.	0.8	44
58	Pattern formation during cubic to orthorhombic martensitic transformations in shape memory alloys. Acta Materialia, 2014, 68, 93-105.	3.8	42
59	A universal symmetry criterion for the design of high performance ferroic materials. Acta Materialia, 2017, 127, 438-449.	3.8	42
60	Influence of nanoscale structural heterogeneity on shear banding in metallic glasses. Acta Materialia, 2017, 134, 104-115.	3.8	42
61	Particle translational motion and reverse coarsening phenomena in multiparticle systems induced by a long-range elastic interaction. Physical Review B, 1992, 46, 11194-11197.	1.1	41
62	Microstructure and transformation texture evolution during α precipitation in polycrystalline α/β titanium alloys – A simulation study. Acta Materialia, 2015, 94, 224-243.	3.8	41
63	Phase-Field Simulation of Orowan Strengthening by Coherent Precipitate Plates in an Aluminum Alloy. Metallurgical and Materials Transactions A: Physical Metallurgy and Materials Science, 2015, 46, 3287-3301.	1.1	41
64	Deformation mechanisms of D022 ordered intermetallic phase in superalloys. Acta Materialia, 2016, 118, 350-361.	3.8	41
65	Ϊ‰-Assisted α nucleation in a metastable β titanium alloy. Scripta Materialia, 2019, 171, 62-66.	2.6	41
66	Influence of Ni4Ti3 precipitation on martensitic transformations in NiTi shape memory alloy: R phase transformation. Acta Materialia, 2021, 207, 116665.	3.8	40
67	Simulating Microstructural Evolution and Electrical Transport in Ceramic Gas Sensors. Journal of the American Ceramic Society, 2000, 83, 2219-2226.	1.9	39
68	Generalized Stacking Fault Energy of Al-Doped CrMnFeCoNi High-Entropy Alloy. Nanomaterials, 2020, 10, 59.	1.9	37
69	Novel transformation pathway and heterogeneous precipitate microstructure in Ti-alloys. Acta Materialia, 2020, 196, 409-417.	3.8	35
70	Non-conventional transformation pathways and ultrafine lamellar structures in Î ³ -TiAl alloys. Acta Materialia, 2020, 189, 25-34.	3.8	34
71	A new mechanism for low and temperature-independent elastic modulus. Scientific Reports, 2015, 5, 11477.	1.6	33
72	Effect of autocatalysis on variant selection of α precipitates during phase transformation in Ti-6Al-4V alloy. Computational Materials Science, 2016, 124, 282-289.	1.4	33

#	Article	IF	CITATIONS
73	Linear-superelastic metals by controlled strain release via nanoscale concentration-gradient engineering. Materials Today, 2020, 33, 17-23.	8.3	33
74	Phase field simulation of martensitic transformation in pre-strained nanocomposite shape memory alloys. Acta Materialia, 2019, 164, 99-109.	3.8	32
75	Extended defects, ideal strength and actual strengths of finite-sized metallic glasses. Acta Materialia, 2014, 73, 149-166.	3.8	31
76	Defect strength and strain glass state in ferroelastic systems. Journal of Alloys and Compounds, 2016, 661, 100-109.	2.8	31
77	Crystallographic analysis and phase field simulation of transformation plasticity in a multifunctional β-Ti alloy. International Journal of Plasticity, 2017, 89, 110-129.	4.1	31
78	A new αÂ+Âβ Ti-alloy with refined microstructures and enhanced mechanical properties in the as-cast state. Scripta Materialia, 2022, 207, 114260.	2.6	31
79	Microstructural evolution during the precipitation of ordered intermetallics in multiparticle coherent systems. Philosophical Magazine A: Physics of Condensed Matter, Structure, Defects and Mechanical Properties, 1995, 72, 1161-1171.	0.7	29
80	High-energy X-ray diffuse scattering studies on deformation-induced spatially confined martensitic transformations in multifunctional Ti–24Nb–4Zr–8Sn alloy. Acta Materialia, 2014, 81, 476-486.	3.8	29
81	Phase-field simulation of twin boundary fractions in fully lamellar TiAl alloys. Acta Materialia, 2012, 60, 6372-6381.	3.8	28
82	Movement of Kirkendall markers, second phase particles and the Type 0 boundary in two-phase diffusion couple simulations. Acta Materialia, 2004, 52, 1917-1925.	3.8	27
83	Integrated Computational Materials Engineering (ICME) Approach to Design of Novel Microstructures for Ti-Alloys. Jom, 2014, 66, 1287-1298.	0.9	27
84	Mechanical behavior and microstructural analysis of NiTi-40Au shape memory alloys exhibiting work output above 400°C. Intermetallics, 2017, 86, 33-44.	1.8	27
85	Ferroic glasses. Npj Computational Materials, 2017, 3, .	3.5	27
86	Large electrocaloric efficiency over a broad temperature span in lead-free BaTiO3-based ceramics near room temperature. Applied Physics Letters, 2017, 111, .	1.5	27
87	Making metals linear super-elastic with ultralow modulus and nearly zero hysteresis. Materials Horizons, 2019, 6, 515-523.	6.4	27
88	Slip transmission assisted by Shockley partials across <mml:math xmlns:mml="http://www.w3.org/1998/Math/MathML" altimg="si1.gif" overflow="scroll"><mml:mrow><mml:mi>α</mml:mi><mml:mo>/</mml:mo><mml:mi>β</mml:mi>interfaces in Ti-alloys. Acta Materialia, 2019, 171, 291-305.</mml:mrow></mml:math 	v>< <mark>ʔ</mark> īħml:n	nath>
89	Implementation of high interfacial energy anisotropy in phase field simulations. Scripta Materialia, 2006, 54, 1919-1924.	2.6	25
90	Finding activation pathway of coupled displacive-diffusional defect processes in atomistics: Dislocation climb in fcc copper. Physical Review B, 2012, 86, .	1.1	25

#	Article	IF	CITATIONS
91	Intrinsic coupling between twinning plasticity and transformation plasticity in metastable β Ti-alloys: A symmetry and pathway analysis. Acta Materialia, 2020, 196, 488-504.	3.8	24
92	H-phase precipitation and its effects on martensitic transformation in NiTi-Hf high-temperature shape memory alloys. Acta Materialia, 2021, 208, 116651.	3.8	24
93	Strain states and unique properties in cold-rolled TiNi shape memory alloys. Acta Materialia, 2022, 231, 117890.	3.8	24
94	A biopolymer-like metal enabled hybrid material with exceptional mechanical prowess. Scientific Reports, 2015, 5, 8357.	1.6	23
95	Determination of twinning path from broken symmetry: A revisit to deformation twinning in bcc metals. Acta Materialia, 2020, 196, 280-294.	3.8	23
96	Predicting grain boundary structure and energy in BCC metals by integrated atomistic and phase-field modeling. Acta Materialia, 2019, 164, 799-809.	3.8	22
97	Novel B19′ strain glass with large recoverable strain. Physical Review Materials, 2017, 1, .	0.9	20
98	Role of point defects in the formation of relaxor ferroelectrics. Acta Materialia, 2022, 225, 117558.	3.8	20
99	Phase field simulation of the stress-induced α microstructure in Ti–6Al–4ÂV alloy and its CPFEM properties evaluation. Journal of Materials Science and Technology, 2021, 90, 168-182.	5.6	19
100	Numerical simulation of irradiation hardening in Zirconium. Journal of Nuclear Materials, 2013, 438, 209-217.	1.3	18
101	Simulation Study of Heterogeneous Nucleation at Grain Boundaries During the Austenite-Ferrite Phase Transformation: Comparing the Classical Model with the Multi-Phase Field Nudged Elastic Band Method. Metallurgical and Materials Transactions A: Physical Metallurgy and Materials Science, 2017, 48, 2730-2738.	1.1	18
102	Finite strain phase-field microelasticity theory for modeling microstructural evolution. Acta Materialia, 2020, 191, 253-269.	3.8	17
103	Phase-field modelling of transformation pathways and microstructural evolution in multi-principal element alloys. Applied Physics Letters, 2021, 119, .	1.5	17
104	Modeling of Dynamical Evolution of Micro/Mesoscopic Morphological Patterns in Coherent Phase Transformations. , 1996, , 325-371.		16
105	A homogenized primary creep model of nickel-base superalloys and its application to determining micro-mechanistic characteristics. International Journal of Plasticity, 2018, 110, 202-219.	4.1	15
106	Three-dimensional phase field simulation of intragranular void formation and thermal conductivity in irradiated α-Fe. Journal of Materials Science, 2018, 53, 11002-11014.	1.7	15
107	Solid solution strengthening of high-entropy alloys from first-principles study. Journal of Materials Science and Technology, 2022, 121, 105-116.	5.6	15
108	Polarization Spinodal at Ferroelectric Morphotropic Phase Boundary. Physical Review Letters, 2020, 125, 127602.	2.9	14

#	Article	IF	CITATIONS
109	Revealing the atomistic mechanisms of strain glass transition in ferroelastics. Acta Materialia, 2020, 194, 134-143.	3.8	14
110	High temperature phase stability of the compositionally complex alloy AlMo0.5NbTa0.5TiZr. Applied Physics Letters, 2021, 119, .	1.5	14
111	Reentrant strain glass transition in Ti-Ni-Cu shape memory alloy. Acta Materialia, 2022, 226, 117618.	3.8	14
112	Effect of nonlinear and noncollinear transformation strain pathways in phase-field modeling of nucleation and growth during martensite transformation. Npj Computational Materials, 2017, 3, .	3.5	13
113	Shearing mechanisms of co-precipitates in IN718. Acta Materialia, 2021, 220, 117305.	3.8	13
114	Self-organized multigrain patterning with special grain boundaries produced by phase transformation cycling. Physical Review Materials, 2018, 2, .	0.9	13
115	Systematic Approach to Microstructure Design of Ni-Base Alloys Using Classical Nucleation and Growth Relations Coupled with Phase Field Modeling. Metallurgical and Materials Transactions A: Physical Metallurgy and Materials Science, 2008, 39, 984-993.	1.1	12
116	Form of critical nuclei at homo-phase boundaries. Scripta Materialia, 2018, 146, 276-280.	2.6	12
117	Heterogeneous <mml:math <br="" altimg="si1.gif" xmlns:mml="http://www.w3.org/1998/Math/MathML">overflow="scroll"><mml:mtext>γâ€2</mml:mtext></mml:math> microstructures in nickel-base superalloys and their influence on tensile and creep performance. International Journal of Plasticity, 2018, 109, 153-168.	4.1	12
118	Tilt strain glass in Sr and Nb co-doped LaAlO3 ceramics. Acta Materialia, 2019, 168, 250-260.	3.8	12
119	Deformation pathway and defect generation in crystals: a combined group theory and graph theory description. IUCrJ, 2019, 6, 96-104.	1.0	12
120	Effect of external stress on \hat{I}^3 nucleation and evolution in TiAl alloys. Intermetallics, 2015, 65, 1-9.	1.8	11
121	Critical nuclei at hetero-phase interfaces. Acta Materialia, 2020, 200, 510-525.	3.8	11
122	Achieving large super-elasticity through changing relative easiness of deformation modes in Ti-Nb-Mo alloy by ultra-grain refinement. Materials Research Letters, 2021, 9, 223-230.	4.1	11
123	Numerical Calculation of Electrical Conductivity of Porous Electroceramics. , 1999, 3, 17-23.		10
124	Quantifying microstructures in isotropic grain growth from phase field modeling: Methods. Acta Materialia, 2012, 60, 4787-4799.	3.8	10
125	Dissecting the influence of nanoscale concentration modulation on martensitic transformation in multifunctional alloys. Acta Materialia, 2019, 181, 99-109.	3.8	10
126	Microstructure development and morphological transition during deposition of immiscible alloy films. Acta Materialia, 2021, 220, 117313.	3.8	10

#	Article	IF	CITATIONS
127	Strain Glass State, Strain Glass Transition, and Controlled Strain Release. Annual Review of Materials Research, 2022, 52, 159-187.	4.3	10
128	Exploration of spinodal decomposition in multi-principal element alloys (MPEAs) using CALPHAD modeling. Scripta Materialia, 2022, 214, 114657.	2.6	10
129	Stress-dependent dislocation core structures leading to non-Schmid behavior. Materials Research Letters, 2021, 9, 134-140.	4.1	9
130	Phase Field Modeling of Microstructural Evolution in Solids: Effect of Coupling among Different Extended Defects. Metallurgical and Materials Transactions A: Physical Metallurgy and Materials Science, 2008, 39, 1630-1637.	1.1	8
131	Quantifying the abnormal strain state in ferroelastic materials: A moment invariant approach. Acta Materialia, 2015, 94, 172-180.	3.8	8
132	Existence of a quadruple point in a binary ferroelectric phase diagram. Physical Review B, 2021, 103, .	1.1	8
133	Harmonic Noise-Elimination Method Based on the Synchroextracting Transform for Magnetic-Resonance Sounding Data. IEEE Transactions on Instrumentation and Measurement, 2021, 70, 1-11.	2.4	8
134	Medium-range ordering, structural heterogeneity, and their influence on properties of Zr-Cu-Co-Al metallic glasses. Physical Review Materials, 2021, 5, .	0.9	8
135	Indirect nucleation in phase transformations with symmetry reduction. Philosophical Magazine A: Physics of Condensed Matter, Structure, Defects and Mechanical Properties, 1996, 74, 1407-1420.	0.7	7
136	Accelerating ferroic ageing dynamics upon cooling. NPG Asia Materials, 2016, 8, e319-e319.	3.8	7
137	Phase Transformation Graph and Transformation Pathway Engineering for Shape Memory Alloys. Shape Memory and Superelasticity, 2020, 6, 115-130.	1.1	7
138	Hidden pathway during fcc to bcc/bct transformations: Crystallographic origin of slip martensite in steels. Physical Review Materials, 2018, 2, .	0.9	7
139	Generalized stacking fault energy surface mismatch and dislocation transformation. Npj Computational Materials, 2021, 7, .	3.5	6
140	Monte Carlo simulation of magnetic domain structure and magnetic properties near the morphotropic phase boundary. Physical Chemistry Chemical Physics, 2017, 19, 7236-7244.	1.3	5
141	On the use of metastable interface equilibrium assumptions on prediction of solidification micro-segregation in laser powder bed fusion. Science and Technology of Welding and Joining, 2019, 24, 446-456.	1.5	5
142	Phase-Field Microstructure Modeling. , 2009, , 297-311.		5
143	3D PHASE FIELD SIMULATION OF EFFECT OF INTERFACIAL ENERGY ANISOTROPY ON SIDEPLATE GROWTH IN Ti6Al4V. Jinshu Xuebao/Acta Metallurgica Sinica, 2013, 48, 148-158.	0.3	5
144	Unique properties associated with normal martensitic transition and strain glass transition – A simulation study. Journal of Alloys and Compounds, 2013, 577, S102-S106.	2.8	4

#	Article	IF	CITATIONS
145	Phase Formation in Ti–Ni Binary System during Solid-State Synthesis. Shape Memory and Superelasticity, 2018, 4, 351-359.	1.1	4
146	Microstructural design for advanced light metals. MRS Bulletin, 2019, 44, 281-286.	1.7	4
147	Cubic martensite in high carbon steel. Physical Review Materials, 2018, 2, .	0.9	4
148	Modeling Dislocation Dissociation and Cutting of γ′ Precipitates in Ni-Based Superalloys by the Phase Field Method. Materials Research Society Symposia Proceedings, 2002, 753, 1.	0.1	3
149	Origin of the modulus anomaly over a wide temperature range of Mn0.70Fe0.25Cu0.05 alloy. Computational Materials Science, 2017, 140, 89-94.	1.4	3
150	Phase Field Simulation of Orowan Strengthening by Coherent Precipitate Plates in a Mg-Nd Alloy. , 2015, , 63-71.		3
151	Modeling and Simulation of Microstructure Evolution during Heat Treatment of Titanium Alloys. , 2016, , 573-603.		3
152	Creep Behavior of Compact γ′-γ″ Coprecipitation Strengthened IN718-Variant Superalloy. Metals, 2021, 11, 1897.	1.0	3
153	Quasiâ€Linear Superelasticity with Ultralow Modulus in Tensile Cyclic Deformed TiNi Strain Glass. Advanced Engineering Materials, 2022, 24, .	1.6	3
154	Pathways to Titanium Martensite. Transactions of the Indian Institute of Metals, 2022, 75, 1051-1068.	0.7	3
155	Novel Characterization of Deformation Mechanisms in a Ni-base Superalloy Using HAADF Imaging and Atomic Ordering Analysis. Microscopy and Microanalysis, 2016, 22, 272-273.	0.2	2
156	A general phase-field framework for predicting the structures and micromechanical properties of crystalline defects. Materials and Design, 2021, 209, 109959.	3.3	2
157	New Insights into Deformation of Metallic Glasses by Combining Mesoscale Simulation and Fluctuation Electron Microscopy. Microscopy and Microanalysis, 2016, 22, 1436-1437.	0.2	1
158	Probing Nanoscale Structural Heterogeneity in Metallic Glasses Using 4-D STEM. Microscopy and Microanalysis, 2018, 24, 202-203.	0.2	1
159	Defect-free plastic deformation through dimensionality reduction and self-annihilation of topological defects in crystalline solids. Physical Review Research, 2020, 2, .	1.3	1
160	\hat{l}_\pm phase growth and branching in titanium alloys. Philosophical Magazine, 0, , 1-24.	0.7	1
161	Coupling Microstructure Characterization with Microstructure Evolution. , 2011, , 151-197.		0
162	Phase Field Model and Computer Simulation of Strain Glasses. Springer Series in Materials Science, 2018, , 253-272.	0.4	0

#	Article	IF	CITATIONS
163	Structure, Morphology and Coarsening Behavior of MX (NbC) Nanoprecipitates in Fe-Ni-Cr Based Alloys. Microscopy and Microanalysis, 2019, 25, 2612-2613.	0.2	0